Precision Fe I and Fe II wavelengths in the red and infra-red spectrum of the iron-neon hollow cathode lamp

G. Nave, R. Learner, J. Murray, A. Thorne, J. Brault

Classification
Physics Abstracts
06.20H—07.50E/G—32.20F/J

Precision Fe I and Fe II wavelengths in the red and infra-red spectrum of the iron-neon hollow cathode lamp

G. Nave ([1]), R.C.M. Learner ([1]), J.E. Murray ([1]), A.P. Thorne ([1]) and J.W. Brault ([2])

([1]) Blackett Laboratory, Imperial College, London SW7 2BZ, G.B.
([2]) National Solar Observatory, P.O.Box 26732, Tucson, Az. 85726 U.S.A.

(Received 30 October 1991, accepted 17 January 1992)

Abstract. — Wavelengths and wavenumbers are presented for 290 lines in the spectrum of the Iron-Neon hollow cathode lamp. The lines are all strong, stable, well resolved lines in Fe I or Fe II; the range covered is from 424 nm to 4.2 μm (23600 to 2354 cm^{-1}). The measurements were made by Fourier transform spectrometry with a wavenumber precision of ± 0.0003 cm^{-1} or better. The absolute accuracy, based on visible region Ar II standards, varies from 0.001 cm^{-1} at 20000 cm^{-1} to 0.0005 cm^{-1} at 2300 cm^{-1}. The absolute scale used is the same as that employed in earlier work, covering the range from 17350 to 55000 cm^{-1}. The intensities, damping parameters (Lorentzian component of line profile) and observed signal to noise ratios of the lines are also tabulated. Auxiliary experiments showed that lines of large Doppler width or high damping parameter suffer significant wavenumber shifts; such lines have been excluded from the list. It is also shown that the wavenumbers of unbroadened lines are the same in large (950 mA, 4 mB) and small (20 mA, 10 mB) hollow cathode lamps.

Introduction.

In two previous papers [1, 2] (papers 1 and 2) we presented recommended standard wavelengths in the Fe-Ne hollow cathode lamp spectrum accurately measured by Fourier transform spectrometry (FTS). Paper 1 covered the range from 382 to 576 nm (26200 to 17350 cm^{-1}) and paper 2 the range 183 to 385 nm (54600 to 26000 cm^{-1}). This paper is an extension of this work into the infrared and presents the wavelengths of 290 well-defined iron lines in the wavelength range from 420 nm to 4.2 μm (23600 cm^{-1} to 2350 cm^{-1})

There are three traditional advantages of FTS over grating spectrometry: multiplex gain, high throughput and high resolution. For photon-noise-limited measurements the multiplex advantage is lost for an absorption spectrum but offers some gain for an emission spectrum, as is the case here. However, the principal benefits for precision wavelength measurement stem from the throughput advantage first pointed out by Jacquinot and the intrinsic linearity of the

FTS wave-number scale. A less publicised but very important characteristic is the approximately constant noise level, which makes it easy to evaluate the signal-to-noise ratio (SNR) for every line in the spectrum and, combined with the Jacquinot advantage, results in a high SNR for strong lines. Since the wavenumber error is determined by the ratio of the line width to the SNR [3], objective estimates of the error of measurement can be made for each individual line, and it is no longer necessary to choose very narrow lines as standards. The classical set of wavelength standards, summarised in reference [4], was determined using either photographic plates or lead sulphide detectors. The maximum SNR for photographic work was limited by the dynamic range of the emulsion to about 30, and it was extremely difficult to improve in this figure; PbS was also a very noisy detector. Effort was therefore directed at reducing line width, either by reducing the temperature (e.g. the Engelhard lamp) or increasing the mass of the emitting atom (e.g., ^{198}Hg or ^{232}Th). In the current FTS work many hundreds of lines have been observed simultaneously with SNRs from 100 to several thousand. It follows that the centres of symmetrical lines can be determined with great precision. Light atoms such as iron (or, in absorption, light molecules such as methane) can therefore provide satisfactory standards.

Current infra-red emission standards.

Previous studies by grating spectrometry of the iron spectrum in the photographic infra-red include the work of Russell, Moore and Weeks [5] and Crosswhite [6]. In the region from 1.1 to 4 μm the spectrum has been observed and analysed by Litzén and Vergès [7]and by Litzén [8] using FTS. A further investigation by Biémont *et al.* [9], extending to 5.5 μm, used an FTS laboratory spectrum to identify iron lines in the solar infra-red spectrum. None of these investigations was used to generate standard wavelengths in the infra-red. The long wavelength limit of Fe I standards based on direct measurement is 571 nm [10]; that for standards derived using the Ritz principle is 577 nm [4].

The availability of standards from elements other than iron at wavelengths longer than 576 nm is best discussed in three ranges: the first is the old "photographic" infra-red, now the region up to the cut-off of the silicon photo-diode at 1.1 μm. This region (see Tab. I) is well supplied with standards of high accuracy: there are roughly a thousand emission line standards between 576 and 1100 nm with precision ranging from 0.3 mK (Ar II) to 2 mK (Th I and II). (1 mK = 0.001 cm^{-1}.) In the next region, the near infra-red from 1.1 to 2.5 μm, there are some two hundred well-determined emission lines, essentially all of which are from the spectra of neutral inert gases. Beyond 2.52 μm, the long wavelength limit of ^{86}Kr in reference [4], fourteen precision wavelengths are listed by Humphreys [11], all of which are inert gas lines.

Since 1974, the date of reference [4], techniques have changed. The most accurate wavelength standards in the infra-red have been generated by frequency multiplication [12, 13] and are based on transitions observed in absorption in the spectra of small molecules. We have decided to present the (less accurate) data in this paper for three reasons. First, the lines are emission lines; problems with wavelength shifts due to changes of illumination (see e.g. paper 1) make it difficult to combine emission and absorption measurements with high absolute accuracy. Second, the spectrum of iron is of dominating astrophysical importance. Third, the measurements combine with those of papers 1 and 2 to give a set of wavelengths from 183 nm to 4.2 μm that are from a single source and on a single consistent scale.

Table I. — *Existing emission line standards in the infra-red. The figures in columns 2, 3 and 4 are the numbers of recommended standard lines in the wavelength range given at the head of the relevant column. The accuracy (column 5) is in units of* mK (0.001 cm^{-1}).

Spectrum	Range, μ m			Accuracy	Ref.
	.576-1.1	1.1-2.5	2.5-5.5		
Ne I	106	23[a]	-	0.6	4
	-	18[b]	7	1.0	11
Si I	35	1	-	1.7	4
Ar I	110	46	-	0.8	4
	178	77	-	0.5	14
	20	3	-	1.0	11
ArII	77	-	-	0.8	4
	158	1	-	0.5	15
CuII	123	-	-	1.4	4
Ge I	20	1	-	1.2	4
^{86}Kr I	82	63	-	0.4	4
^{136}Xe I	-	8	7	1.0	11
Th I & II	253	-	-	2.0	4

a) all at $\lambda < 1.8$ μm
b) all at $\lambda > 1.8$ μm

Experimental details.

The experimental procedures are similar to those of papers 1 and 2, and only a brief description is given here. The light source used was a continuously pumped hollow cathode lamp run in neon or argon. The cathode was a cylinder of pure iron 8 mm in bore and 35 mm long. The optimum gas pressure in neon was 5 mbar with currents between 0.5 and 1.4 A. For most of the observations the cathode was uncooled, but some infra-red data were taken with a water cooled cathode. At the high lamp currents used the principal gain from cooling is the suppression of unwanted continuum radiation; the linewidths decreased by less than 10 % . The operating conditions for all the spectra used are summarised in table II. With the exception of B1, B2 and C1 they were recorded with the $f/55$ IR-visible-UV FTS at the National Solar Observatory, Tucson. The interferograms typically contained 10^6 points and were asymmetrically truncated with a 1:4 ratio between the negative and positive path differences, giving a resolution step of 10 to 20 mK. The range covered was from 1850 to 11000 cm^{-1}, and the cathode was focused on the input aperture of the FTS. Two wide-range bridging spectra (B1 and B2) were

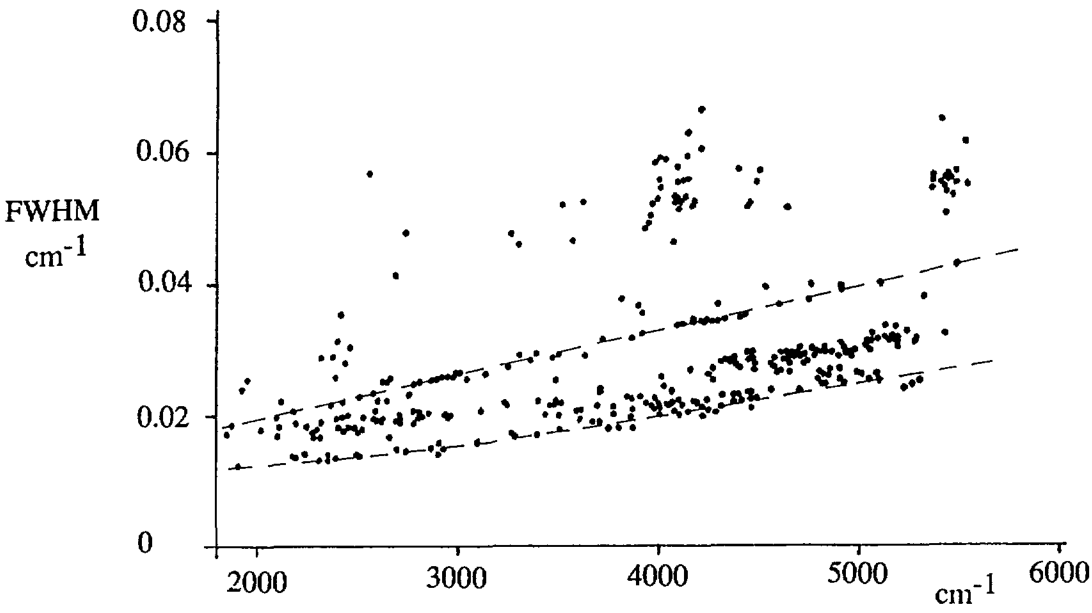

Fig.1. — Observed width (FWHM in mK) for all strong lines in spectrum N6 plotted against wavenumber. The dotted lines indicate the trend for Gaussian lines in Neon (upper line) and Iron (lower line). The points clustered above the lower line come from the iron lines rejected on account of a large Lorentzian component or an anomalously large Doppler width.

also recorded in order to link the infra-red spectra with visible spectra calibrated from Ar II standards (paper 1) so as to put the two sets of measurements on the same absolute scale and fill the gap in the line list. These bridging spectra were recorded with the $f/25$ VUV-visible FTS at Imperial College. The interferograms contained 5 x 10^5 points and were symmetrically truncated, giving a resolution step of 30 mK.

All spectra were carefully phase corrected by the methods outlined in paper 2, and all suitable (symmetric and unblended) lines of good signal-to-noise ratio were then subjected to detailed analysis. Voigt profiles were fitted to these lines, using the suite of programs "DECOMP" developed by Brault [14]. For lines that have a near-Gaussian profile the minimum observed line width increases from 16 mK at 2100 cm^{-1} to 90 mK at 18000 cm^{-1}, corresponding to a Doppler temperature of between 2000 and 2500 K (see Fig. 1). Many of the lines in the infra-red, especially the majority of the neon lines and the iron lines involv ing states with f and g electrons, have profiles with a significant Lorentzian component. Such lines are not suitable for precision measurement. In the case of Neon the broadening is associated with pressure and current shifts of between -16 and $+\ 40$ mK, while the lines that are not seriously broadened are precisely those that are expected to show asymmetries due to isotope shifts; we do not therefore include any neon data in the final list.

Calibration and line selection.

The linearity of the FTS wavenumber scale makes it possible to calibrate a complete spectrum from a set of reference lines at one end of it. The calibration from the set of Ar II lines adopted as absolute standards in paper 1 can therefore be carried both into the ultra-violet (paper 2) and into the infra-red, as is done in this paper. The method is described in paper 1. The difference $\Delta\sigma$ between the wavenumbers of a set of suitable lines in the spectrum to be calibrated and the reference spectrum is evaluated. A plot of $\Delta\sigma/\sigma$ against σ then gives a horizontal straight line whose offset from zero is the calibration constant to be applied.

The first attempts to calibrate from the visible to 5 μm proved unsatisfactory: alternative routes (e.g., calibrating spectrum N1 from spectrum N3 *via* either N2 or N6) gave results that were inconsistent by several times the calculated errors. Closer examination showed there to be at least two, and probably three, different populations within the iron spectrum. These groups show systematic current-dependent shifts with respect to one another and, fortunately, can be distinguished by differences in Doppler width. We have not seriously attempted to identify these populations, partly because many of the lines are not classified, but it seems likely that most of the anomalous lines are either Fe II lines or Fe I lines arising from ion-electron recombination. If the choice of lines for calibration is restricted to those from the lowest width group, we obtain a set of calibration constants that is consistent for all possible routes. The earlier inconsistency was due to the random samples of the different populations that occurred in each overlap region. In the following discussion and in the recommended wavenumber table, we restrict ourselves entirely to lines from the low width, internally consistent population.

The error of an individual calibration step depends on the observed rms value of $\Delta\sigma/\sigma$ and the number of lines used. Figure 2 shows an example of the scatter in $\Delta\sigma/\sigma$ for one pair of spectra. In most cases the standard error of the mean was in the range 3 to 10 parts per billion (ppb). The longest calibration sequence - from the wavenumbers of paper 1 to the far infra-red spectrum N1 - required 4 calibration steps. The errors of these steps can be combined in the usual way, and in table II, we give the cumulative errors rounded up to conservative values. The increase in relative error as the calibration sequence gets longer is nearly balanced by the decrease in wavenumber, so that the absolute calibration error throughout the range of table III is between 0.1 and 0.2 mK.

Several of the spectra used in this work were observed with the cathode imaged on the entrance aperture of the spectrometer. This geometry can introduce illumination shifts, but we showed in Paper 1 that any such shift was less than 20 ppb (0.5 mK at 22000 cm^{-1}). Combining this with the 0.35 mK uncertainty in the original Ar II standards and the above calibration errors gives a total uncertainty in the calibration constant that changes only slightly over the whole region, from 0.6 mK in the visible to 0.4 mK at 3000 cm^{-1}

Having calibrated the spectra, we come to the selection of lines for the recommended wavelength list. As already remarked, many of the iron lines in the infra-red are susceptible to pressure broadening and have line profiles with a significant Lorentzian component; this is characterized by the damping parameter, the ratio of the half width of the Lorentzian to the total half width. We have compared lines from two spectra with different damping - one taken with argon as the carrier gas and the other with Neon. Figure 3 shows that the scatter in $\Delta\sigma/\sigma$ increases when the damping parameter becomes large (> 0.5) and there is a barely significant upward trend. Damping parameters (and therefore sensitivity to current and pressure) are lower with Neon as carrier gas, and run-to-run reproducibility is better. Nonetheless we have eliminated all lines for which the damping parameter (in Neon) is greater than 0.33 before compiling the list of recommended lines. We have also eliminated the lines of large Doppler width that were found to be unsuitable for calibration purposes.

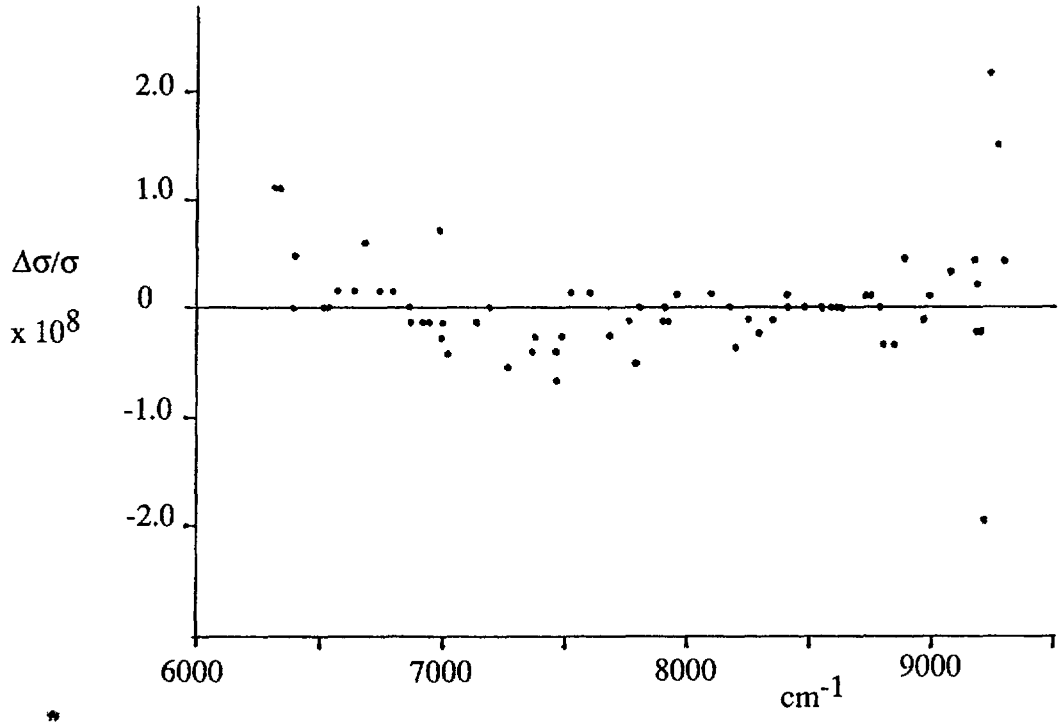

Fig.2. — The ratio of wavenumber differences to wavenumber ($\Delta\sigma/\sigma$) for all strong, well-resolved lines in the two spectra N2 and N6 plotted against the the wavenumber.

In papers 1 and 2, we discussed several minor effects on precision at the 10 or 20 parts per billion level: these include pressure, illumination, cathode alignment, optical depth, phase errors and the number of points in the FFT algorithm. Analysis of the spectra used in this paper show that there are no observable wavelength shifts associated with change of cathode temperature. We have also investigated the effect of large changes in lamp current and cathode size on the lines in our final list by comparing a typical low current commercial (Rank-Hilger) Iron-Neon hollow cathode lamp with our usual source. The smaller lamp runs at 20 mA and 10 mB with a single-ended cathode of diameter 2.5 mm and depth 15 mm. Comparison of the wave numbers of a few hundred strong ultra-violet FeI lines from the stable (low Doppler width) population between the spectrum C1 from this lamp and spectra previously taken with the high current lamp showed agreement to an rms error of $\pm$ 5x10^9 (0.2 mK at 40000 cm^{-1}). The uncertainty with which high and low current lamp spectra can be set on the same scale is therefore negligible compared to other sources of error, and the energy levels involved in these transitions are evidently not affected by the change of lamp.

The final decisions required in the selection of a recommended set of wavelengths are a related pair: the number of lines required and the minimum acceptable signal-to-noise ratio. The rule that the precision with which the position of a well resolved line can be determined is given by the ratio of line width (FWHM) to twice the signal-to-noise ratio [3] implies for our spectra that a precision of $\pm$ 0.2 mK requires lines with SNR $>$ 50 at 2500 cm^{-1}, rising to SNR $>$ 250 at 20000 cm^{-1} Selection by these criteria would yield a very large number of lines, heavily biased towards the region between 5000 and 7000 cm^{-1} In practice we have

Table II. — *Experimental data for spectra used. Spectrum N6 was taken with a water-cooled hollow cathode; all others were uncooled. Spectrum* B2 *is in two parts, with a gap from* 13500 *to* 17500 cm^{-1}, *the region of the strong neon lines. The last column gives for each spectrum the cumulated error (in ppb) for the calibration transfer from paper* 1.

Ref.	Wavenumber range (cm^{-1})	Carrier gas	Press. (mB)	Current (mA)	Resolution mK*	Cum. calib. error (ppb)
N1	1750-5600	Ne	5.3	850	9.5	25
N2	3750-9000	Ne	5.3	860	11.9	20
N3	7700-11000	Ne	5.5	1050	15.4	20
N6	1850-9000	Ne	3.7	1400	11.9	20
B1	9000-15000	Ne	6.0	500	30.1	10
B2	9000-23000+	Ne	6.0	850	35.0	5
C1	34000-55000	Ne	≈ 10	20	62.2	-

* 1 mK = 0.001 cm^{-1}
+ with gap from 13500 to 17500 cm^{-1}

chosen the SNR limits to give a more uniform distribution of lines. The SNR cut-off has been set at 50 for $\sigma < 4000$ cm^{-1} and at 200 for $\sigma > 20000$ cm^{-1} Between these limits it has been varied between 100 and 200 so as to maintain a roughly even line density. The exception is the region between 13500 and 17500 cm^{-1} where the extremely strong neon lines contribute so much noise to the spectrum that very few iron lines have high SNR.

Recommended wavelengths.

The list of recommended lines is presented in table III. Column 1 gives the directly measured vacuum wavenumber. When this has been obtained from two or more independent spectra (column 6), column 1 gives the weighted mean and column 2 the rms deviation. Columns 3, 4, 5 and 7 show the intensity (arbitrary units), the FWHM (mK), the damping (ratio of Lorentzian FWHM to total FWHM) and the SNR respectively. The intensities are on a consistent relative scale calibrated for instrument response against a tungsten lamp, but must be regarded as a guide only: the hollow cathode is far from local thermodynamic equilibrium, and relative intensities vary with running conditions. Column 8, the air wavelength, is calculated from column 1 and the refractive index of air and is discussed further below.

The relative precision of the wavenumber measurement for an individual line estimated from its SNR is confirmed by the run-to-run reproducibility indicated in column 2. The mean value for this column through the whole list is less than ± 0.2 mK, but at the short wavelength end, where many lines appear on only one spectrum, it is more realistic to take ± 0.5 mK. As already discussed, the absolute accuracy of the calibration, including uncertainties in the Ar II standards and possible illumination shifts, improves slightly from 0.6 mK in the visible to 0.4 mK in the infra-red. Combining the calibration uncertainty with the run-to-run reproducibility yields a final accuracy that can be conservatively specified as ranging from ±1.0 mK at 23000 cm^{-1} (40 ppb) to ± 0.5 mK at 2300 cm^{-1} (200 ppb). The corresponding variation in wavelength accuracy is 0.2 mÅ at 4300 Å to 10 mÅ at 4.3 μm. For this reason the wavelength is given to only three places of decimals for wavelengths above 2 μm.

It should be borne in mind that the wavelength in "standard air" (column 8) is derived from the observed vacuum wavenumber using Edln's 1966 dispersion formula [16] for air. Both this and the 1953 dispersion formula [17] are based on measurements at or below 2.06 μm, and

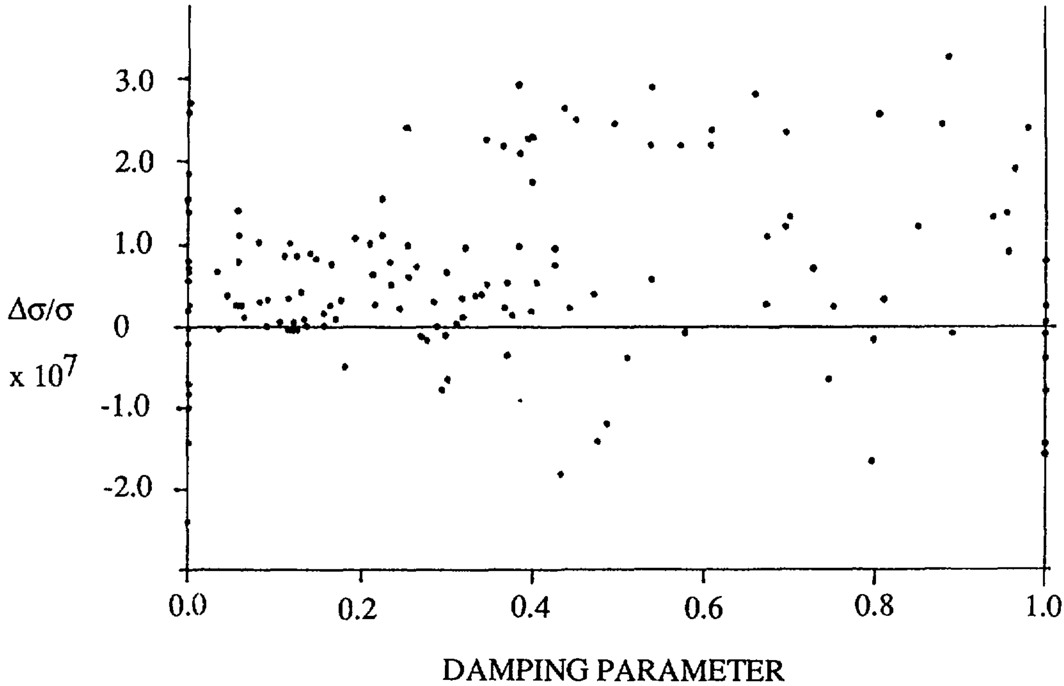

Fig.3. — $\Delta\sigma/\sigma$ for strong Iron lines in spectra N2 and A2 plotted against the damping parameter in spectrum N2. The damping parameter is the ratio of Lorentzian FWHM to total FWHM in the fitted Voigt profile.

we have extrapolated beyond this limit when compiling table III - as is also done in the NBS Table of Wavenumbers [18]. Although correction terms for changes in CO_2 concentration and for non-zero humidity are available [19], neither the main dispersion formula nor the correction terms make any allowance for the dispersive effects of the strong infra-red absorption bands of CO_2 and H_2O. These effects may be greater than the divergence of the two formulae in the near infra-red, where the 1953 formula is consistently below, and the 1965 formula above, the experimental refractive index measurements. At 5 μm the difference between the two extrapolations is 0.7 mÅ. We can only repeat Edlén's 1953 comment: "of existing refractivity observations in the infra-red there is none that can be judged sufficiently accurate to furnish any improvement on extrapolation from the [recommended dispersion] formula."

Table III includes 20 lines that overlap with the long wave length end of the list in paper 1. These measurements are completely independent of the earlier ones and were indeed made after a gap of several years and with a different instrument and a different source. It is encouraging to find that the rms deviation between the two sets is only 0.2 mK.

Figure 4 shows a comparison of our Fe I wavelengths with those of Litzén and Vergès [7]. The mean difference is 100 ppb and the standard deviation is ± 400 ppb, which is more than an order of magnitude greater than the run-to-run reproducibility of our spectra. These differences are consistent with the estimate of Litzén and Vergès of 1-10 mK for their wavenumber accuracy. Comparison with the work of Biémont *et al.* [9] is also reassuring. Their laboratory spectrum is one of the set included in this work, but their calibration used the strong Ar I lines in the near infra-red and applied a different phase correction algorithm. The two

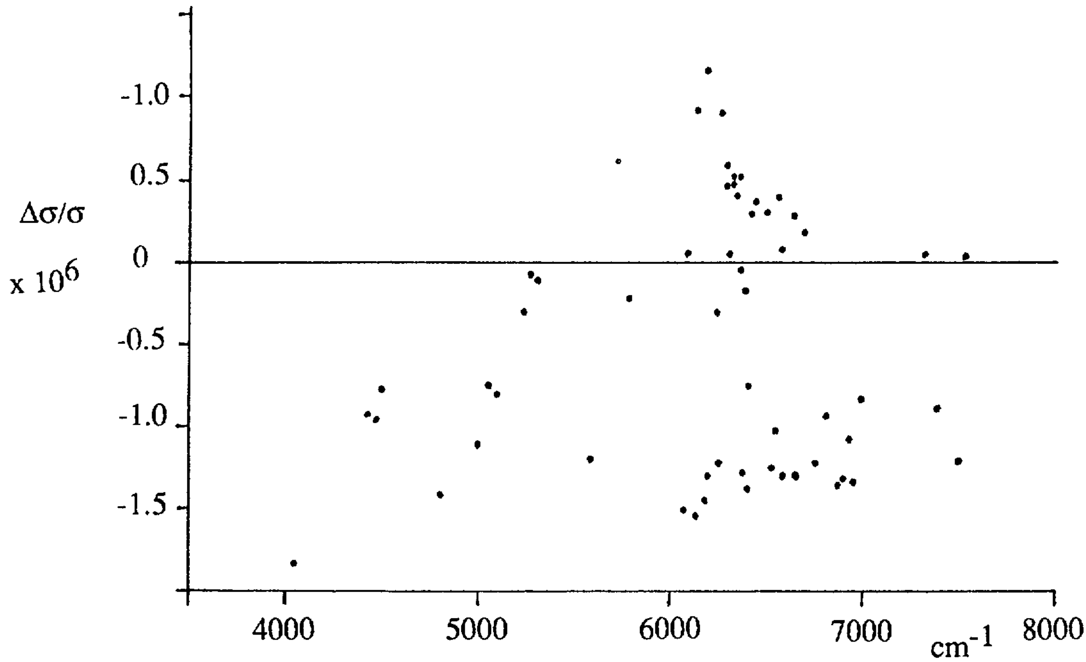

Fig.4. — Comparison of wavenumbers from table 3 with the data of Litzén and Vergès [7]. $\Delta\sigma/\sigma$ for the two sets of wavenumbers is plotted against σ.

scales agree to one mK at the long wavelength end of the range (2300 cm^{-1}) and two mK at the other end (9000 cm^{-1}).

Conclusions.

The list presented in table III completes our work on well-determined lines in the iron spectrum and underlines the superiority of FTS for this type of measurement. Between them, papers 1 and 2 plus the current work present about 1100 lines of good quality set on a single scale with an accuracy of the order of one mK. There are a host of small effects at the level of a few ten thousandths of a wave number that suggest higher accuracy to be unrealistic in a multi-line emission spectrum. In effect we are unable to realise the ideal of an isolated atom. This view is confirmed by the rigour of the definition of the ^{86}Kr wavelength standard where fastidious control of every parameter of the lamp is needed to attain a reproducibility only a factor of three better than that achieved in the present work.

Acknowledgments.

We thank SERC for a grant in support of the work reported here and for a studentship held by J.E.M. We also thank Mr.G.Cox for his continued skilled assistance throughout the work on the iron spectrum.

Table III. — *Recommended wavenumbers for strong, well-resolved lines emitted by the iron-neon hollow cathode lamp. Column 1: the observed vacuum wavenumber in units of* cm^{-1} *or the weighted mean if* $N \geq 2$. *Column 2: the rms difference (if* $N \geq 2$ *between different spectra in units of mK* ($0.001\ cm^{-1}$). *Column 3: The mean intensity in arbitrary units, roughly corrected for instrument response. Column 4: the FWHM, in mK, of the Voigt profile fitted to the line. Column 5: the damping parameter - i.e., the ratio of the Lorentzian FWHM to the total FWHM of the fitted Voigt profile. Column 6: the number N of independent observations of the line. Column 7: the observed signal-to-noise ratio for the line or the square root of the sums of the squares if* $N \geq 2$. *Column 8: the air wavelength derived from column 1 and the dispersion formula of reference* [16].

Wavenumber	Delsig	Int	FWHM	Damping	No.	SNR	Air-Wavelength
2354.4189		190	13	.00	1	76	42461.746
2500.3719		250	14	.00	1	84	39983.146
2696.0566		550	15	.01	1	160	37081.096
2789.0518	.35	17	16	.03	2	60	35844.703
2905.2555	.12	19	17	.11	2	59	34410.995
3102.1162	.09	27	17	.13	2	100	32227.268
3253.9934	.00	23	18	.00	2	150	30723.089
3750.0293	.09	120	18	.09	2	460	26659.184
3755.8537	.10	110	18	.07	2	650	26617.843
3799.9900		310	18	.22	1	240	26308.680
3812.5448		320	18	.00	1	1900	26222.045
3939.0001	.10	29	22	.32	2	120	25380.228
3983.3376	.00	12	23	.31	2	57	25097.727
3983.4372	.03	11	21	.32	2	53	25097.100
4042.7154	.14	67	22	.27	2	320	24729.101
4072.5481	.14	49	22	.29	2	230	24547.953
4219.1754	.18	17	21	.17	2	100	23694.847
4242.1230	.28	21	22	.18	2	120	23566.671
4319.4842	.25	19	23	.25	2	100	23144.596
4406.7654		30	26	.30	1	170	22686.189
4419.6929	.21	100	22	.17	2	690	22619.833
4448.5159	.25	36	23	.24	2	220	22473.273
4466.8971	.25	58	22	.17	2	420	22380.796
4491.1011	.23	18	23	.26	3	130	22260.179
4561.2024		17	27	.31	1	100	21918.064
4632.1181		26	28	.33	1	160	21582.505
4662.7181		81	28	.33	1	490	21440.865
4708.5184		16	27	.32	1	100	21232.307
4722.8336		16	28	.30	1	100	21167.951
4783.2143		42	29	.30	1	260	20900.738
4796.9685	.42	19	25	.20	3	160	20840.810
4820.9337		44	29	.31	1	270	20737.209
4823.0879		66	28	.29	1	420	20727.947
4828.8336		32	28	.30	1	200	20703.283
4981.4973		42	29	.30	1	250	20068.807
5051.2025	.18	63	26	.14	4	1500	19791.8628
5056.4586	.00	29	29	.32	2	210	19771.2895
5091.4767	.16	27	26	.15	4	660	19635.3067
5166.1408		39	30	.28	1	220	19351.5255
5186.8861		120	30	.27	1	700	19274.1277

Table III (*continued*)

Wavenumber	Delsig	Int	FWHM	Damping	No.	SNR	Air-Wavelength
5230.4272	.18	34	25	.06	4	780	19113.6786
5238.1377		61	31	.32	1	320	19085.5433
5265.3210	.16	68	25	.12	4	1400	18987.0102
5283.2502		39	30	.27	1	210	18922.5760
5301.7223	.21	120	25	.11	4	2500	18856.6465
5301.7223	.21	120	25	.11	4	2500	18856.6465
5364.0224	.37	8	24	.10	4	210	18637.6369
5492.7978	.44	14	30	.30	3	290	18200.6882
5523.1511	.23	23	30	.19	2	340	18100.6635
5573.2964	.16	18	28	.19	3	380	17937.8040
5575.6731	.17	28	29	.20	3	570	17930.1578
5601.9773	.14	15	31	.33	3	270	17845.9663
5704.6774	.10	22	31	.19	2	280	17524.6888
5748.6432	.14	15	32	.18	2	200	17390.6593
5766.6674	.09	16	32	.17	2	220	17336.3033
5772.8208	.14	18	32	.18	2	230	17317.8241
5777.0785	.10	17	32	.12	3	260	17305.0608
5777.9948	.01	29	30	.18	3	560	17302.3165
5803.8912	.18	24	30	.13	3	390	17225.1152
5825.5382	.22	18	30	.18	3	350	17161.1087
5876.9098	.10	26	31	.27	3	470	17011.0988
5878.8623	.15	18	30	.16	3	360	17005.4490
5888.9773	.14	55	32	.18	2	690	16976.2402
5913.1772	.10	16	31	.25	3	230	16906.7642
5931.6334	.10	18	30	.23	2	230	16854.1590
5946.8765	.10	26	31	.14	4	550	16810.9581
6056.6395	.09	11	31	.19	3	220	16506.2969
6068.4828	.18	11	30	.21	3	210	16474.0831
6082.3127	.04	14	31	.28	2	240	16436.6244
6094.6380	.15	13	27	.19	3	280	16403.3843
6124.1048	.19	30	30	.17	3	580	16324.4575
6126.2653	.28	13	30	.31	3	240	16318.7005
6171.7233	.17	32	30	.12	3	670	16198.5045
6189.0144	.13	22	30	.15	3	450	16153.2485
6232.4563	.04	57	32	.32	2	900	16040.6558
6233.5567	.26	12	32	.27	3	200	16037.8242
6244.5400	.13	28	30	.12	3	570	16009.6158
6262.0424	.09	32	32	.28	2	530	15964.8689
6268.1221		63	34	.31	1	270	15949.3839
6279.4354	.26	15	34	.31	3	260	15920.6488
6283.1236	.22	37	32	.27	2	610	15911.3033
6285.2009	.26	45	32	.26	3	820	15906.0446
6296.1239	.17	24	32	.26	2	390	15878.4495
6300.0612	.17	56	32	.28	2	900	15868.5260
6318.2596	.30	52	32	.31	3	940	15822.8201

Table III (*continued*)

Wavenumber	Delsig	Int	FWHM	Damping	No.	SNR	Air-Wavelength
6320.1279	.26	180	32	.26	2	3000	15818.1427
6323.3281	.16	10	31	.15	3	210	15810.1372
6339.6527	.27	240	33	.24	3	4000	15769.4261
6350.7263	.32	31	33	.18	3	590	15741.9293
6358.1328	.13	78	32	.24	3	1400	15723.5917
6370.6285	.14	29	31	.12	3	600	15692.7505
6383.1296	.18	58	33	.24	3	1000	15662.0169
6384.7607	.10	23	35	.32	2	250	15658.0158
6388.6369	.22	19	31	.16	3	380	15648.5155
6395.4072	.18	110	31	.15	3	2200	15631.9497
6399.6200	.04	180	33	.27	2	3000	15621.6593
6432.3865	.13	19	33	.28	2	310	15542.0827
6436.6622	.26	18	33	.17	3	350	15531.7585
6493.5366	.31	33	33	.22	3	610	15395.7216
6493.9789	.26	52	33	.28	2	860	15394.6730
6519.0845	.13	75	32	.17	3	1500	15335.3866
6536.4850	.13	410	32	.18	3	4400	15294.5628
6557.7470	.31	57	33	.22	3	1000	15244.9736
6568.6700	.23	60	34	.26	3	1100	15219.6228
6573.8929	.13	130	32	.18	3	2700	15207.5310
6610.9081	.22	22	33	.28	3	420	15122.3822
6630.6796	.15	20	33	.29	3	370	15077.2899
6641.9309	.13	180	32	.17	3	3600	15051.7492
6684.3851	.18	65	34	.19	3	1200	14956.1517
6742.8776	.13	190	33	.18	3	4000	14826.4113
6748.1927	.05	16	32	.29	3	320	14814.7335
6791.7792	.23	39	33	.16	3	860	14719.6592
6799.4896	.09	82	33	.15	3	1700	14702.9676
6863.4566	.18	62	34	.18	3	1200	14565.9366
6868.5956	.18	230	34	.20	3	4100	14555.0385
6888.8674	.18	330	34	.20	3	4200	14512.2075
6922.2269	.18	89	34	.18	3	1800	14442.2704
6924.4777	.09	11	31	.14	3	250	14437.5759
6942.2858	.18	440	34	.21	3	4500	14400.5411
6993.9042	.23	15	34	.18	3	330	14294.2580
6998.3948	.23	110	34	.18	3	2300	14285.0859
7015.0022	.11	15	35	.31	3	290	14251.2672
7022.4154	.27	160	35	.22	3	3400	14236.2228
7070.4454	.15	16	38	.16	2	240	14139.5151
7121.1319	.09	5	34	.19	2	100	14038.8733
7137.1888	.23	57	36	.23	3	1000	14007.2892
7193.7433	.14	49	36	.23	3	890	13897.1690
7231.4775	.28	7	32	.25	3	140	13824.6528
7267.6365	.20	37	36	.20	3	710	13755.8703
7314.3650	.10	11	32	.24	3	230	13667.9895
7369.8858	.23	86	36	.22	3	1700	13565.0220

Table III (*continued*)

Wavenumber	Delsig	Int	FWHM	Damping	No.	SNR	Air-Wavelength
7379.7020	.06	23	35	.25	3	470	13546.9783
7465.0458	.23	47	37	.22	3	1000	13392.1028
7466.5418	.28	16	37	.29	3	340	13389.4195
7487.3683	.22	27	36	.19	3	600	13352.1761
7523.2413	.05	4	34	.02	3	120	13288.5089
7523.6260	.14	17	34	.09	3	410	13287.8295
7539.0018	.08	7	37	.23	3	170	13260.7289
7603.6857	.22	11	38	.21	3	250	13147.9208
7686.2507	.21	10	35	.08	3	240	13006.6868
7740.0266	.10	12	35	.27	3	280	12916.3192
7761.9918	.12	18	36	.07	3	400	12879.7680
7795.2230	.18	8	36	.04	3	190	12824.8612
7806.0038	.10	7	35	.22	3	150	12807.1488
7903.7626	.08	24	38	.12	3	510	12648.7415
7910.0385	.06	57	38	.16	3	1100	12638.7059
7961.5087	.05	6	37	.10	3	130	12556.9980
8067.0248	.25	9	36	.24	3	190	12392.7530
8099.5980	.10	9	39	.16	3	180	12342.9145
8176.3087	.14	12	39	.12	3	250	12227.1121
8201.1346	.23	5	36	.21	3	110	12190.0990
8294.3620	.10	11	39	.15	3	220	12053.0838
8327.3061	.27	9	42	.29	3	170	12005.3999
8349.8053	.07	2100	38	.14	3	5000	11973.0503
8384.7203	.17	33	38	.13	3	720	11923.1930
8412.3119	.00	430	39	.14	3	4400	11884.0859
8413.1892	.05	1100	39	.13	3	4700	11882.8467
8484.2882	.04	710	39	.11	3	4600	11783.2673
8551.9959	.03	450	39	.14	3	4400	11689.9768
8589.9952	.04	320	39	.14	3	4200	11638.2641
8612.7061	.05	500	39	.13	3	4600	11607.5750
8622.3814	.09	10	40	.12	3	200	11594.5499
8623.0946	.04	170	40	.15	3	3300	11593.5910
8752.3900	.04	91	40	.13	3	1600	11422.3233
8848.0260	.16	50	41	.08	3	980	11298.8621
8885.5743	.12	98	42	.08	3	2100	11251.1157
8966.7459	.13	16	41	.07	3	300	11149.2646
8985.8245	.27	13	40	.21	3	230	11125.5925
9185.0589	.00	15	43	.32	2	220	10884.2651
9202.5978	.18	13	45	.22	2	200	10863.5211
9203.3325	.05	14	43	.11	2	220	10862.6539
9271.2727	.50	9	45	.11	2	150	10783.0518
9297.1775	.11	13	43	.15	2	220	10753.0068
9492.0593		60	45	.27	1	600	10532.2359
9519.8365		33	45	.18	1	350	10501.5046
9564.2380		41	45	.31	1	440	10452.7517
9616.6367		17	46	.10	1	200	10395.7971
9667.7010		9	47	.06	1	110	10340.8868
9783.5766		12	48	.08	1	170	10218.4102

Table III (*continued*)

Wavenumber	Delsig	Int	FWHM	Damping	No.	SNR	Air-Wavelength
9853.8244	.23	83	50	.07	3	1300	10145.5630
9932.6524	.11	62	48	.31	3	1000	10065.0451
9999.6601	.06	69	53	.15	2	940	9997.5990
10109.4368	.25	31	53	.12	2	520	9889.0364
10137.4224		34	54	.30	1	510	9861.7364
10200.9636		15	52	.18	1	270	9800.3080
10211.3521		15	56	.19	1	250	9790.3377
10239.0039		16	52	.19	1	290	9763.8975
10250.3481	.04	22	52	.04	2	440	9753.0916
10265.6304	.02	110	54	.08	2	2100	9738.5723
10356.5091	.23	33	54	.10	2	690	9653.1157
10385.1459	.29	26	53	.25	3	510	9626.4974
10446.5560	.06	27	54	.08	2	590	9569.9078
10462.3331		10	55	.13	1	210	9555.4764
10508.7586		16	54	.18	1	360	9513.2622
10526.2295		8	53	.06	1	200	9497.4725
10574.4137		11	54	.16	1	260	9454.1954
10586.0507	.09	20	58	.10	2	470	9443.8026
10601.4347	.42	33	53	.11	3	780	9430.0984
10619.5159	.05	27	54	.20	3	630	9414.0423
10634.1205	.15	18	57	.08	2	450	9401.1133
10666.1332	.10	44	52	.10	3	1000	9372.8972
10678.1359		10	51	.06	1	300	9362.3617
10691.7760	.10	25	49	.20	3	660	9350.4175
10692.9480		11	57	.13	1	270	9349.3927
10745.5492		16	59	.09	1	410	9303.6257
10753.2992		10	59	.04	1	270	9296.9205
10805.7566		24	60	.10	1	600	9251.7877
10811.8671		14	52	.06	1	420	9246.5589
10830.1565	.23	44	55	.06	2	1300	9230.9437
10849.4857	.07	14	54	.29	2	340	9214.4980
10861.1298		16	59	.09	1	420	9204.6192
10861.7459		66	60	.12	1	1700	9204.0971
10881.7417		25	60	.08	1	660	9187.1840
10892.5589		44	60	.09	1	1100	9178.0603
10895.0982	.12	50	61	.18	2	1300	9175.9212
10895.8572		7	57	.16	1	200	9175.2820
10914.9325	.05	28	54	.32	2	810	9159.2469
10930.5869	.17	26	56	.06	2	720	9146.1293
10947.0355		54	60	.09	1	1400	9132.3867
10951.5876		17	54	.13	1	510	9128.5907
10958.3752	.01	42	61	.04	2	1200	9122.9365
10963.2485		26	51	.06	1	820	9118.8812
10966.4107	.41	24	58	.11	2	630	9116.2517
10971.4915	.40	34	54	.30	3	940	9112.0300
10994.5368		10	55	.13	1	290	9092.9305

Table III (*continued*)

Wavenumber	Delsig	Int	FWHM	Damping	No.	SNR	Air-Wavelength
10998.5640		8	56	.00	1	250	9089.6011
10998.8022	.25	51	56	.10	2	1500	9089.4042
11000.1160	.03	97	55	.04	3	2900	9088.3186
11003.6247		4	58	.08	1	110	9085.4206
11009.9359	.42	9	53	.32	2	240	9080.2126
11010.7024	.27	24	55	.02	3	690	9079.5805
11015.6056		27	60	.16	1	680	9075.5390
11031.7706		5	54	.21	1	130	9062.2405
11034.4789		11	55	.11	1	320	9060.0162
11078.0658		18	55	.16	1	430	9024.3693
11081.7964		10	56	.16	1	250	9021.3313
11083.2349		10	55	.12	1	240	9020.1604
11088.3606		13	55	.22	1	300	9015.9907
11093.1787	.12	50	58	.08	2	1100	9012.0748
11108.6087	.02	400	57	.03	2	4400	8999.5568
11165.2380		16	60	.11	1	160	8953.9115
11199.3255		28	61	.08	1	110	8926.6583
11311.1223	.10	130	58	.00	2	210	8838.4287
11329.3341		820	61	.00	1	620	8824.2210
11369.1168	.14	120	57	.03	2	190	8793.3432
11407.2267	.05	98	58	.00	2	150	8763.9658
11416.0562	.38	110	58	.00	2	180	8757.1875
11506.1398	.24	1800	59	.00	2	2800	8688.6256
11524.5483	.00	200	58	.00	2	320	8674.7470
11608.7796	.19	120	54	.00	2	200	8611.8043
11742.0346	.14	140	59	.01	2	200	8514.0724
11805.3520	.05	170	60	.00	2	250	8468.4074
11918.8408	.10	710	61	.00	2	960	8387.7726
11998.7442	.05	120	59	.00	2	170	8331.9155
12005.7466	.00	590	61	.00	2	790	8327.0559
12161.5463	.10	440	60	.00	2	590	8220.3788
12364.9204	.24	95	61	.00	2	120	8085.1721
12425.0456	.19	130	61	.00	2	180	8046.0475
12498.2107	.09	180	61	.00	2	240	7998.9453
12581.7304	.28	250	61	.01	2	340	7945.8467
12764.2984	.19	170	63	.00	2	230	7832.1965
12849.0147	.00	140	63	.00	2	190	7780.5569
13178.5174	.19	150	64	.00	2	210	7586.0185
13310.1059	.10	360	66	.01	2	470	7511.0200
13338.4360	.05	240	66	.00	2	320	7495.0669
13426.7820	.00	140	66	.01	2	190	7445.7503
13870.8295		150	65	.03	1	180	7207.3878
13909.5621		220	66	.01	1	280	7187.3179
17797.4733		1100	101	.00	1	200	5617.2158
18156.8432		450	90	.00	1	100	5506.0357
18971.7187		440	94	.07	1	180	5269.5372

Table III (*continued*)

Wavenumber	Delsig	Int	FWHM	Damping	No.	SNR	Air-Wavelength
19125.4149		270	94	.10	1	120	5227.1895
19346.3725		500	97	.02	1	300	5167.4883
20165.4367		230	104	.01	1	390	4957.5966
20317.4542		150	102	.04	1	300	4920.5028
20437.9520		93	102	.06	1	200	4891.4922
22406.9302		120	108	.05	1	250	4461.6528
22580.7391		270	110	.05	1	400	4427.3099
22643.0693		620	112	.01	1	780	4415.1225
22696.3876		1600	120	.00	1	2000	4404.7503
22845.8671		450	111	.02	1	430	4375.9297
23110.8162		3700	126	.00	1	2000	4325.7619
23168.0012		700	113	.04	1	240	4315.0845
23253.4122		590	115	.06	1	260	4299.2347
23281.0835		1200	112	.02	1	300	4294.1247
23344.8070		1300	115	.02	1	340	4282.4029
23402.9660		6500	124	.00	1	1800	4271.7605
23464.9611		1400	121	.00	1	710	4260.4742
23518.4354		3200	116	.02	1	550	4250.7869
23522.1290		1300	116	.02	1	220	4250.1194
23600.8831		720	117	.09	1	270	4235.9368

References

[1] Learner R.C.M. and Thorne A.P., Wavelength calibration of Fourier-transform emission spectra with applications to Fe I, *J. Opt. Soc. Am.* **B5** (1988) 2045-2059.

[2] Nave G., Learner R.C.M., Thorne A.P. and Harris C.J., Precision Fe I and Fe II wavelengths in the ultra-violet spectrum of the Iron-Neon hollow cathode lamp, *J. Opt. Soc. Am.* **B8** (1991) 2028-2041.

[3] Brault J.W., High precision Fourier transform spectrometry. *Mikrochim. Acta* (Wien) **1987 III** (1988) 215-227.

[4] Kaufman V. and Edlén B., Reference wavelengths from atomic spectra in the range 15-25000A *J. Phys. Chem. Ref. Data* **3** (1974) 825-895.

[5] Russell H.N., Moore C. and Weeks D., The spectrum of Iron I. *Trans. Am. Phil. Soc.* **34** (1944) 113-179.

[6] Crosswhite H., The iron-neon hollow-cathode spectrum. *J. Res. Nat. Bur. Stand.* (US) **79A** (1975) 17-69

[7] Litzén U. and Vergès J., The Fe I spectrum in the region $1-4$ μm *Phys. Scr.* **13** (1976) 240-244.

[8] Litzén U., New levels and classifications in Fe I. *Phys. Scr.* **14** (1976) 165-169.

[9] Biémont E., Brault J.W., Delbouille L. and Roland G., An investigation of iron in the infra-red solar spectrum based on FTS laboratory measurements. *Astron. Astrophys. Suppl. Ser.* **61** (1985) 107-125.

[10] Stanley R.W. and Dieke G.H., Interferometric wavelengths from a hollow cathode discharge. *J. Opt. Soc. Am.* **45** (1955) 280-286.

[11] Humphreys C.J., First spectra of neon, argon and xenon in the 1.2- 4.0 μm region. *J. Phys. Chem. Ref. Data* **2** (1973) 519-529.

[12] Jennings D.J.E., Evenson K.M. and Knight D.J.E., Optical frequency measurements. *Proc. IEEE.* **74** (1986) 168-178.

[13] Guelachvili G. and Narahari Rao K., Handbook of Infra-red Standards, (Academic Press, London, 1986).

[14] Brault J.W. and Abrams M.C., DECOMP: a Fourier transform spectra decomposition program. Tech. Dig. Ser. (Opt. Soc. Am.) **6** (1989) 110-112.

[15] Norlén G., Wavelengths and energy levels of Ar I and Ar II based on new interferometric measurements in the region 3400-9800 *Phys. Scr.* **8** (1973) 249-269.

[16] Edlén B., The refractive index of air *Metrologia* **2** (1966) 71-80.

[17] Edlén B., The dispersion of standard air *J. Opt. Soc. Am.* **43** (1953) 339-344.

[18] Coleman C.D., Bozman W.R. and Meggers W.F., Tables of Wavenumbers, **II**, 7000A to 100μm National Bureau of Standards (USA), Monograph 3, 1960.

[19] Owens J.C., Optical refractive index of air: dependence on pressure, temperature and composition Appl. Opt. **6** (1967) 51-59.